

LA-4165

C.3<sup>m</sup>

CIC-14 REPORT COLLECTION  
REPRODUCTION  
COPY

LOS ALAMOS SCIENTIFIC LABORATORY  
of the  
University of California  
LOS ALAMOS • NEW MEXICO

Measurement of  
Pyrocarbon Thermal Conductivity  
by the Fission Couple Method

LOS ALAMOS NATIONAL LABORATORY



3 9338 00382 1161

UNITED STATES  
ATOMIC ENERGY COMMISSION  
CONTRACT W-7405-ENG 36

## LEGAL NOTICE

This report was prepared as an account of Government sponsored work. Neither the United States, nor the Commission, nor any person acting on behalf of the Commission:

A. Makes any warranty or representation, expressed or implied, with respect to the accuracy, completeness, or usefulness of the information contained in this report, or that the use of any information, apparatus, method, or process disclosed in this report may not infringe privately owned rights; or

B. Assumes any liabilities with respect to the use of, or for damages resulting from the use of any information, apparatus, method, or process disclosed in this report.

As used in the above, "person acting on behalf of the Commission" includes any employee or contractor of the Commission, or employee of such contractor, to the extent that such employee or contractor of the Commission, or employee of such contractor prepares, disseminates, or provides access to, any information pursuant to his employment or contract with the Commission, or his employment with such contractor.

This report expresses the opinions of the author or authors and does not necessarily reflect the opinions or views of the Los Alamos Scientific Laboratory.

Printed in the United States of America. Available from  
Clearinghouse for Federal Scientific and Technical Information  
National Bureau of Standards, U. S. Department of Commerce  
Springfield, Virginia 22151

Price: Printed Copy \$3.00; Microfiche \$0.65

Written: March 31, 1969  
Distributed: July 18, 1969

LA-4165  
UC-80, REACTOR  
TECHNOLOGY  
TID-4500

**LOS ALAMOS SCIENTIFIC LABORATORY**  
of the  
**University of California**  
LOS ALAMOS • NEW MEXICO

Measurement of  
Pyrocarbon Thermal Conductivity  
by the Fission Couple Method

by

**Peter G. Salgado**

**Fred P. Schilling**

**Gerald T. Brock**



TABLE OF CONTENTS

|   | <u>Page</u> |
|---|-------------|
| I. Introduction.....                    | 1           |
| II. Fabrication of Fission Couples..... | 3           |
| III. Experiments.....                   | 5           |
| IV. Analysis.....                       | 8           |
| V. Results.....                         | 10          |
| VI. Sources of Error.....               | 11          |
| VII. Discussion.....                    | 15          |
| VIII. Acknowledgments.....              | 15          |
| IX. References.....                     | 16          |

LIST OF TABLES

|     |   |    |
|-----|---|----|
| I   | Coated Fuel Particles Used for the Experiments.....                           | 3  |
| II  | Physical Property Data Used in the Analysis.....                              | 3  |
| III | Particle Identification Numbers, Weight, Burst Series,<br>and Dimensions..... | 7  |
| IV  | Type II Particle Thermal Conductivities.....                                  | 12 |
| V   | Type III Particle Thermal Conductivities.....                                 | 12 |
| VI  | Type IV Particle Thermal Conductivities.....                                  | 13 |

LIST OF FIGURES

|    |  |    |
|----|--|----|
| 1  | Photomicrograph of coated particles.....   | 2  |
| 2  | Microradiographs of coated particles used for thermal<br>conductivity determinations.....      | 5  |
| 3  | Fission couple made with bead IV-3.....  | 5  |
| 4  | Bundle of fission couples; side view, end view, and packaged<br>in polyethylene container..... | 5  |
| 5  | Fission couple package centered in housing.....  | 6  |
| 6  | Sandia Pulsed Reactor II.....  | 6  |
| 7  | Oscilloscopes with cameras and amplifiers.....   | 6  |
| 8  | Magnetic tape recorder system and analog-to-digital converter.....                             | 7  |
| 9  | Pulse shape derived by two independent methods.....  | 9  |
| 10 | S-curve fit, pulse shape, and effect on the model of three<br>bare bead responses.....         | 9  |
| 11 | Cooling curve for heat transfer coefficient calculations.....                                  | 10 |
| 12 | Effect on the calculated buffer response of varying the<br>thermal conductivity.....           | 10 |
| 13 | Examples of the model agreement with experimental data.....                                    | 11 |
| 14 | Model agreement with McEachern's results.....  | 13 |
| 15 | Model solutions with the Crank-Nicholson equation and with<br>the Crandall equation.....       | 13 |
| 16 | Effect of doubling the number of nodal points.....   | 13 |
| 17 | Effect of heating in the coat.....   | 14 |

# MEASUREMENT OF PYROCARBON THERMAL CONDUCTIVITY

## BY THE FISSION COUPLE METHOD

by

Peter G. Salgado  
Fred P. Schilling  
Gerald T. Brock<sup>‡</sup>

### ABSTRACT

A technique for measuring the thermal conductivity of the pyrocarbon coatings of coated particle fuel is described. The nuclear fuel particles are overcoated with tungsten, and thermocouple wires are welded 180° apart to the tungsten. These intrinsic thermocouples (fission couples) are subjected to neutron bursts and the surface temperature responses are monitored. If particle dimensions and burst shape are known, the effective thermal conductivity of the pyrocarbon coats can be calculated.

Experiments have been conducted to measure the conductivity of a low-density pyrocarbon buffer coat. Comparisons were made between values obtained by the fission couple method and the xenon flash method for two dense pyrocarbons. A TRISO I particle was tested and the thermal conductivity of the buffer layer was estimated to be  $0.0039 \pm 0.0011$  cal/cm-sec-°C.

### I. INTRODUCTION

The fuel for a High-Temperature Gas-Cooled Reactor (HTGR)<sup>(1)</sup> consists of microspheres of uranium or uranium-thorium carbide (or oxide) encapsulated in two or more layers of pyrocarbon plus, in many cases, a silicon carbide layer. These fuel particles and similar fertile particles are bonded into fuel sticks approximately 1/2-in. in diameter. The fuel element is a hexagonal graphite block which contains a large number of fuel sticks; helium coolant is conducted through holes parallel to the fuel sticks.

A typical fuel particle, which is being considered for the Fort St. Vrain reactor,<sup>(2)</sup> has a spherical (Th,U)C<sub>2</sub> kernel of 200-μm-diameter, a 50-μm buffer layer of low density pyrocarbon, a 17.5-μm layer of SiC, and a 50-μm outer layer of dense, isotropic pyrocarbon. Figure 1 shows a typical particle. The inner, low-density layer protects the outer layers from fission recoil damage, allows the kernel to swell, and collects fission gases. The combination of SiC and dense pyrocarbon outer layers acts as a miniature pressure vessel for retention of fission products.

<sup>‡</sup>Associated Western Universities, June-September 1968; currently with General Electric, San Jose, California.

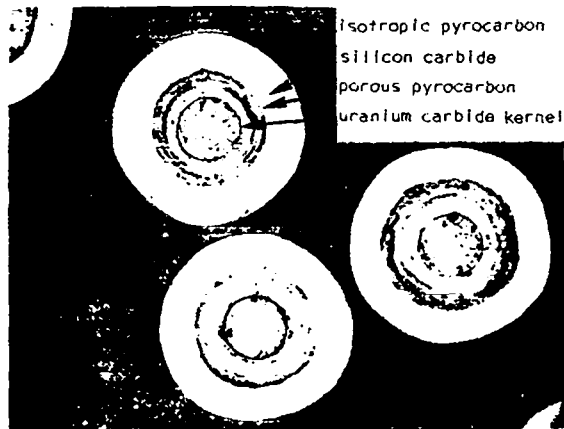


Fig. 1. Photomicrograph of coated particles (100X).

Analysis of the dynamic response of an HTGR depends explicitly on the heat capacities, thermal conductivities, and heat transfer coefficients used in the thermal analysis and the various temperature reactivity feedback mechanisms. Within the coated particles, the rate at which heat is transferred from the fuel to the surrounding matrix and graphite materials is highly dependent on the thermal conductivity of the low-density pyrocarbon buffer layer. This work was done to investigate the possibility of measuring directly the thermal conductivity of the buffer layer of a coated particle.

It was proposed by McEachern<sup>(3)</sup> that the thermal conductivity of the buffer layer in a coated particle could be measured from observation of the surface temperature response of a particle subjected to a rapid neutron burst. The surface temperature is measured by an intrinsic thermocouple (fission couple) composed of a fuel particle coated with a thin layer of tungsten to which thermoelements are welded.

By comparison of the observed surface temperature response of a particle of known dimensions subjected to a known neutron burst, with the calculated surface response for assumed values of thermal conductivity, the effective thermal conductivity can be selected.

Fission couples composed of six particle types were prepared for the experiments described in this report. Bare  $UC_2$  particles and bare uranium-metal particles were used to determine the neutron burst

shape and resulting heat generation rate in the fuel particle. Two types of dense pyrocarbon were deposited on  $UC_2$  cores and in disc form for comparison of measurements of thermal conductivity by the fission couple method and xenon flash method. Particles consisting of core plus buffer layer (a porous, sooty type of pyrocarbon) were prepared for measurement of buffer conductivity. A TRISO<sup>‡</sup> particle, Fig. 1, was tested to measure the effective conductivity of several deposited layers in series and to check whether the values of conductivity determined from the other particles could be used successfully for predicting TRISO particle response.

#### Reported Thermal Conductivity of Pyrocarbon Coatings

In 1967, in the Super Kukla reactor facility at the Nevada Test Site, P. G. Salgado and D. J. Stillman made initial fission couple experiments, which were analyzed by McEachern.<sup>(3)</sup> These experiments indicated that the thermal conductivity of buffer pyrocarbon was  $0.0015 \pm 0.0005$  cal/sec-cm-°C. The reliability of the value was not known because of the limited experience with the fission couple technique and because comparison values were not available. There were also experimental difficulties in selecting the time base and in describing the burst shape.

For two porous pyrocarbons with densities of 1.04 and 0.91 g/cm<sup>3</sup>, Gulf General Atomic reported thermal conductivities of 0.0057 and 0.0074 cal/cm-sec-°C,<sup>(4)</sup> respectively.

Goeddel and Mills<sup>(5)</sup> also reported a thermal conductivity of 0.01 cal/cm-sec-°C for low temperature isotropic (LTI) pyrocarbon coatings. The Gulf General Atomic measurements were made by the xenon flash technique using material deposited on graphite supports.<sup>(4)</sup>

Isotropic pyrocarbon, having the same physical properties as the TRISO LTI material, exhibited a thermal conductivity of 0.020 cal/cm-sec-°C<sup>(6)</sup> as measured by the xenon flash method.<sup>(7)</sup> Although the thickness of the available sample (0.28 mm) was outside the range of applicability for this technique<sup>(8)</sup>, a correction factor based on experience was applied. This material was the disc-shaped isotropic pyrocarbon

<sup>‡</sup>Gulf General Atomic (GGA) nomenclature for particles containing buffer, SiC, and isotropic pyrocarbon layers.

prepared during the same coating run as the isotropic coated particles used in these experiments.

A similar but nonisotropic, disc-shaped, dense pyrocarbon, prepared during the same coating run as the dense pyrocarbon particles used in these experiments, was found to have a thermal conductivity of 0.038 cal/cm-sec-°C.<sup>(9)</sup>

TABLE I  
COATED FUEL PARTICLES USED

| Particle Type | Particle Description   |
|---------------|--|
| I             | <u>Nonisotropic or Dense:</u> UC <sub>2</sub> kernel (93% enriched <sup>235</sup> U) plus 200-μm dense pyrocarbon coat plus 1-μm tungsten coat.  |
| II            | <u>Isotropic:</u> UC <sub>2</sub> kernel (93% enriched <sup>235</sup> U) plus 200-μm isotropic carbon coat plus 3-μm tungsten coat.  |
| III           | <u>Buffer:</u> UC <sub>2</sub> kernel (93% enriched <sup>235</sup> U) plus 40-μm sooty carbon coat plus 3-μm tungsten coat.  |
| IV            | <u>TRISO:</u> 2.2:1 ThC <sub>2</sub> /UC <sub>2</sub> kernel (93% enriched <sup>235</sup> U) plus successive coatings of buffer pyrocarbon, silicon carbide, isotropic pyrocarbon, and 3-μm tungsten coat. |
| V             | <u>Bare:</u> UC <sub>2</sub> kernel (93% enriched <sup>235</sup> U) plus 3-μm of dense pyrocarbon plus 3-μm tungsten coat.   |
| VI            | <u>Metal:</u> U kernel (93% enriched <sup>235</sup> U) with no coatings.   |

## II. FABRICATION OF FISSION COUPLES

The six types of particles fabricated into fission couples are listed in Table I. Pulse shapes and heat transfer coefficients were derived from Type V and Type VI particle responses. Pyrocarbon thermal conductivities were obtained from Type I, Type II, and Type III particles; and the accuracy of these values was tested by predicting the TRISO particle (Type IV) responses using an altered form of the model. The physical property data used are listed in Table II.

### Particle Production

With the exception of the TRISO particles (Type IV above) all particles used in the experiment were prepared at LASL. The 93%-enriched UC<sub>2</sub> kernels were prepared from Gulf General Atomic's cores by stripping the proeutectic carbon shells in a fluidized bed with crushed aluminum oxide. Nonisotropic or dense particles<sup>(10)</sup> (Type I).

Two grams of UC<sub>2</sub> particles, having an average diameter of 165 μm, were combined with 18.6 g of carrier in the form of depleted, carbon-bed UC<sub>2</sub> having a diameter range from 104 to 124 μm. A 50-μm layer of dense pyrocarbon was deposited on the particles at a rate of approximately 45 μm per h at 1400°C from a methane-helium mixture at 2.63 l(STP)/min in an uncooled, 1-in.-diam graphite coater. The methane concentration was increased from 20% to as high as 64% in up to ten steps to maintain a nearly constant deposition rate.

A series of four coating runs provided the 200-μm coating necessary. Between runs the carrier

TABLE II  
PHYSICAL PROPERTY DATA USED IN THE ANALYSIS

| Material Used in the Analysis | Density (g/cm <sup>3</sup> ) | Heat Capacity <sup>‡</sup> (cal/g-°C)                             | Thermal Conductivity (cal/cm-sec-°C) |
|-------------------------------|------------------------------|---|--------------------------------------|
| Uranium Carbide               | 10.9                         | 0.0637 + (0.787 x 10 <sup>-5</sup> ) $\bar{T}$ + 563/ $\bar{T}^2$ | 0.078                                |
| Dense PyC                     | 1.74*                        | 0.25**  | ---                                  |
| Isotropic PyC                 | 1.89                         | 0.25**  | 0.020                                |
| Porous PyC                    | 1.2***                       | 0.25**  | ---                                  |
| Silicon Carbide               | 2.5****                      | 0.288   | 0.04                                 |
| Tungsten                      | 18.5                         | 0.0312 - (4.13 x 10 <sup>-6</sup> ) $\bar{T}$                     | 0.41                                 |

<sup>‡</sup> $\bar{T}$  [=]°K

\*This value was later determined to be 1.89.

\*\*Assumed value.

\*\*\*This value was later determined to be 1.15.

\*\*\*\*This value was later determined to be 3.17.

was screen-separated from the dense pyrocarbon coated particles and fresh, uncoated carrier particles were added to return the bed surface area to 1100 cm<sup>2</sup>. After each separation the coated particles were checked for residual carrier particles by microradiography; the cores were readily distinguishable.

Subsequent metallographic examination indicated variations in surface appearance within each coating increment but these are not believed to indicate a significant variation in physical properties. The examination indicated no separations within the coatings.

#### Isotropic particles<sup>(11)</sup> (Type II).

The isotropic carbon coating was deposited in four steps of 50 μm each in a 1200°C bed, fluidized with 2.63 l(STP)/min of 40% acetylene in helium. The carbon was deposited at a rate of 115 to 130 μm/hr. The entire bed was composed of UC<sub>2</sub> particles (34.3 g and a surface area of 1100 cm<sup>2</sup>) during the first increment. In the subsequent increments, 2 g of UC<sub>2</sub> particles were combined with 28 g of fresh 147 to 175-μm-diam carbon-bed particles. The initial bed surface area for each increment was maintained at 1100 cm<sup>2</sup>. The UC<sub>2</sub> particles were screen-separated after the last three increments. The coating had an average thickness of 199 μm, was optically isotropic, and had a density of 1.89 g/cm<sup>3</sup>.

#### Buffer particles<sup>(12)</sup> (Type III).

Ten grams of the UC<sub>2</sub> cores, having particle diameters from 158 to 170 μm, were coated with porous pyrocarbon for 80 sec from 100% acetylene at 1000°C. Two grams of the product in the 208- to 296-μm range were coated with 3 μm of 1.6 g/cm<sup>3</sup> pyrocarbon from a 2.63 l(STP)/min flow of 20% methane in helium at 1400°C in a fluidized bed with an initial bed surface area of 1100 cm<sup>2</sup>. (The sealing pyrocarbon, necessary to restrict corrosion of the UC<sub>2</sub> by the highly deleterious HF during subsequent tungsten coating, had a preferred orientation index M of about 3.)

#### TRISO particles (Type IV).

Two grams of TRISO-I particles were supplied for this experiment by Gulf General Atomic. Although production methods are proprietary the following characteristics are available.

#### Kernel

|             |             |
|-------------|-------------|
| Composition | 2.25:1 Th:U |
| Size        | 200 μm      |

#### Buffer

|           |                        |
|-----------|------------------------|
| Thickness | 46 μm                  |
| Density   | 1.15 g/cm <sup>3</sup> |

#### SiC

|           |                        |
|-----------|------------------------|
| Thickness | 20 μm                  |
| Density   | 3.17 g/cm <sup>3</sup> |

#### Isotropic

|                         |                        |
|-------------------------|------------------------|
| Type                    | LTI                    |
| Thickness               | 48 μm                  |
| Density                 | 1.93 g/cm <sup>3</sup> |
| Bacon anisotropy factor | 1.06                   |

#### Bare UC<sub>2</sub> particles (Type V).

Two grams of UC<sub>2</sub> particles were coated with 3 to 5 μm of 1.6 g/cm<sup>3</sup> pyrocarbon in the same manner as the sealing coat which was applied to the buffer particles.

#### Metal uranium particles (Type VI).

The spheres of metal uranium were fabricated by the calcium reduction of enriched U<sub>3</sub>O<sub>8</sub>. A large excess of calcium chloride was mixed with U<sub>3</sub>O<sub>8</sub> in a steel bomb and heated inductively. A large increase in bomb surface temperature indicated when the exothermic reaction was completed. The uranium particles were separated from slag, water washed, cleaned with dilute acetic acid, and polished with dilute nitric acid. The particles were sized by wet sieving into fractions of 250 to 500 μm, 500 to 1190 μm, 1190 to 1680 μm, and +1680 μm. The particles for this experiment were selected from the smallest size fraction.

#### Tungsten Coat<sup>(13)</sup>

Layers of tungsten 1 to 5-μm-thick were overcoated on all particle types except Type VI, the metallic uranium. The tungsten was deposited from a fluidized bed by the hydrogen reduction of tungsten hexafluoride in an argon carrier. The bed temperature was maintained at 800 to 1000°C at a pressure of 150 Torr for the 10-min coating period.

#### Fission Couple Fabrication

Approximately 50 particles of each type (except Type VI) were weighed and radiographed. Those 10 to 15 beads of each group which appeared to be most spherical were selected for fabrication into fission couples. The radiographs of those chosen are shown in Fig. 2.

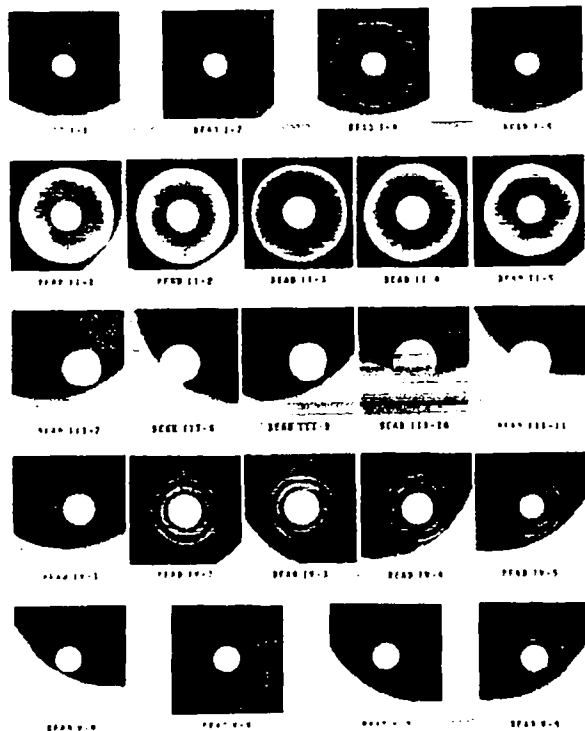


Fig. 2. Microradiographs of coated particles used for thermal conductivity determinations.

The fission couples were fabricated by welding 0.001-in.-diam Chromel and constantan thermocouple wire 180° apart on the surface of the 0.16 to 0.6-mm-diam particles (Fig. 3). The bead was placed onto a grooved aluminum plate for welding; the wire to be attached was laid across the bead, and welding electrodes were pressed down upon the wire at the point of contact with the bead. A constant voltage was applied for approximately 10 msec; the voltage for different particles varied from 0.75 to 0.90 V. The second wire was similarly attached.

Two posts, 0.030-in. Chromel and constantan, were snugly fitted into the 0.0320-in.-diam holes of a 2-in. length of aluminum oxide insulation. The bead was mounted between the posts by welding the fine wires to the spur of corresponding metal. The posts were held in place by an epoxy cement applied to the insulation holes at the end opposite the bead.

### III. EXPERIMENTS

#### The Fission Couple Package

A 1-in.-diam bundle (Fig. 4) was made by taping the ceramic insulators of the fission couples together so that particles were in approximate planar alignment. The bundle was placed in a cardboard

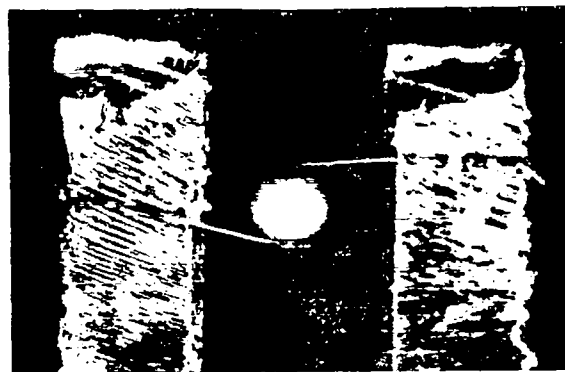


Fig. 3. Fission couple made with Bead IV-3.

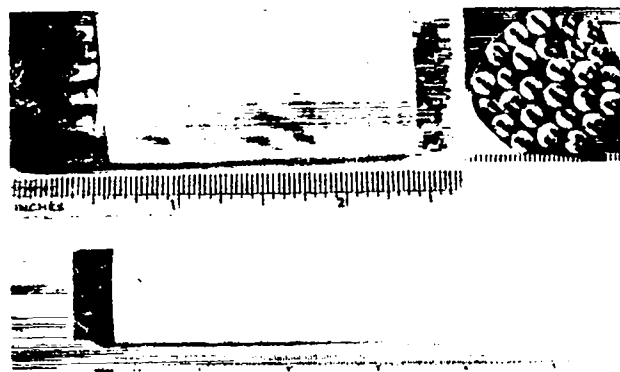


Fig. 4. Bundle of fission couples; side view, end view, and packaged in polyethylene container.

cylinder that extended 1/8-in. beyond the plane of the particles to prevent them from touching the bottom of a polyethylene container. The polyethylene container, designed to increase the thermal neutron flux, was a 1.5-in. o.d., 5-in.-long cylinder with a 2-in.-thick bottom. The cavity was 1.0-in.-diam and 3-in. deep. The package was inserted in an aluminum tube which fitted into the reactor core.

During preliminary experiments the particles faced the reactor from within an open cadmium cylinder. Early estimates had indicated that temperature rises sufficient for this experiment could be attained alongside the reactor. The cadmium was intended to absorb neutrons reflected from the building walls to minimize burst widths. Unfortunately, the cadmium reduced the thermal neutron density so that the observed bead temperature rise was insufficient. The package was relocated in the highest neutron flux available, inside the center sample port. The cadmium cylinder was retained during the first series of experiments, but was later removed.

### The Reactor Facility

The SPR-II (Sandia Pulsed Reactor) fuel assembly, <sup>(14,15)</sup> a right cylinder 8.205-in.-high by 8.078-in.-diam, has a 1.650-in.-diam void (or "glory hole") through the center. The hole accommodates an aluminum housing which positions experiments and prevents debris from accumulating in the core. The core consists of 104 kg of 90 wt% enriched uranium (93.15%)/10 wt% molybdenum alloy. A reactivity insertion of \$0.16 is sufficient to produce a total burst yield of  $1.9 \times 10^{17}$  fissions and  $10^{15}$  n/cm<sup>2</sup> fast neutron flux at the core center. The pulse width at one-half maximum power (fuel temperature of 280°C) is 32  $\mu$ sec.

The reactivity worth of polyethylene inserted into the core is nearly constant over 4 in. The neutron flux, which peaks slightly below the core's geometric center because of voids above the control rods, is generally higher in the bottom than in the top half of the core. <sup>(15)</sup> The fission couples were positioned as close to the geometric center as possible.

The fission couple package was placed in the aluminum tube assembly (Fig. 5). The assembly was carefully aligned over the glory hole so that, as the reactor was raised from the pit, the aluminum

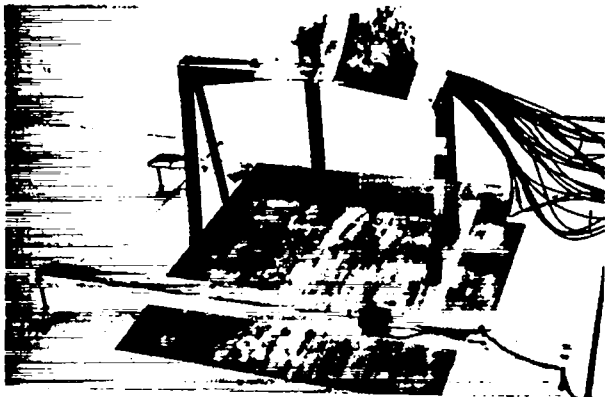


Fig. 5. Fission couple package centered in housing.

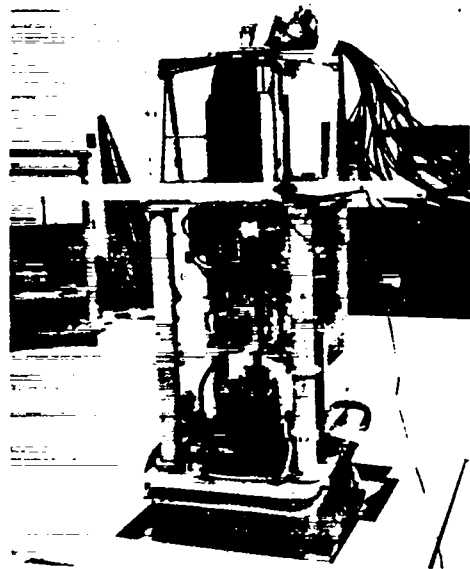


Fig. 6. Sandia Pulsed Reactor II.

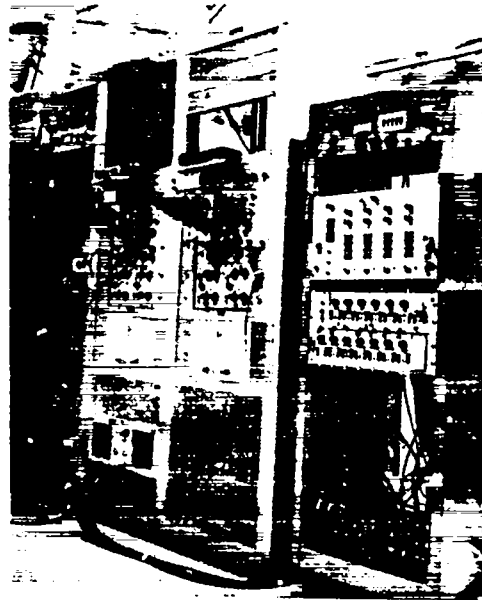


Fig. 7. Oscilloscopes with cameras and amplifiers.

The instrumentation (Figs. 7 and 8) for recording data was located adjacent to the reactor. Data were recorded on magnetic tape, reviewed on an oscilloscope, digitized, and punched on computer cards.

Prior to each series of bursts, the differential amplifiers were adjusted to zero by shorting the

input and monitoring the signal with a digital voltmeter. The amplifier gain was checked with a calibrated millivolt input source. Fission couple continuity was confirmed by measuring circuit resistance at the amplifier input. System calibration was performed by feeding known signals at the fission couple end of the cables and checking the punched card output.

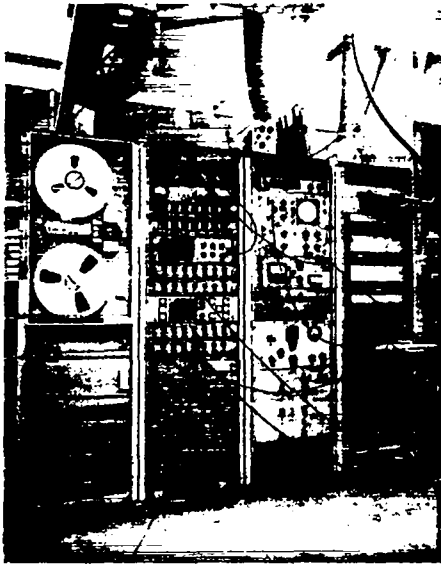


Fig. 8. Magnetic tape recorder system and analog-to-digital converter.

The number of fission couple responses which could be observed during a reactor burst was limited by the number of tape recorder channels. Of the 15 channels available, one was reserved for voice, another recorded the trigger, and, often, two or three more were inoperable.

The particles used in each burst series and their dimensions are listed in Table III; bursts 750 through 758 were series A, bursts 759 through 761 were series B, and bursts 802 through 809 were series C.

TABLE III  
PARTICLE IDENTIFICATION NUMBERS, WEIGHT, BURST SERIES, AND DIMENSIONS

| Particle | Weight (mg) | Burst Series, Response Recorded | Average Core Diam ( $\mu\text{m}$ ) | Average Coating Thicknesses ( $\mu\text{m}$ ) |      |     |      |
|----------|-------------|---------------------------------|-------------------------------------|---|------|-----|------|
|          |             |                                 |                                     | Noniso.                                       | Buff | SiC | Iso. |
| I-1      | 0.174       | A                               | 157                                 | 198   | -    | -   | -    |
| I-2      | 0.174       | A, B                            | 162                                 | 198   | -    | -   | -    |
| I-4      | 0.178       | B                               | 159                                 | 198   | -    | -   | -    |
| I-5      | 0.177       | -                               | 613                                 | 200   | -    | -   | -    |
| II-1     | 0.296       | A, C                            | 186                                 | -   | -    | -   | 208  |
| II-2     | 0.304       | A, C                            | 200                                 | -   | -    | -   | 197  |
| II-3     | 0.303       | B                               | 208                                 | -   | -    | -   | 195  |
| II-4     | 0.320       | B, C                            | 210                                 | -   | -    | -   | 200  |
| II-5     | 0.261       | C                               | 171                                 | -   | -    | -   | 206  |
| III-7    | 0.472       | A, C                            | 161                                 | -   | 36   | -   | -    |
| III-8    | 0.049       | A, C                            | 159                                 | -   | 46   | -   | -    |
| III-9    | 0.032       | A, B, C                         | 155                                 | -   | 40   | -   | -    |
| III-10   | 0.031       | A, C                            | 183                                 | -   | 38   | -   | -    |
| III-11   | 0.030       | B                               | 159                                 | -   | 51   | -   | -    |
| IV-1     | 0.107       | A, C                            | 215                                 | -   | 42   | 20  | 37   |
| IV-2     | 0.126       | -                               | 214                                 | -   | 34   | 22  | 44   |
| IV-3     | 0.126       | A, C                            | 214                                 | -   | 38   | 24  | 36   |
| IV-4     | 0.117       | B                               | 199                                 | -   | 43   | 21  | 35   |
| IV-5     | 0.078       | B                               | 159                                 | -   | 45   | 15  | 46   |
| V-4      | 0.030       | A                               | 161                                 | -   | -    | -   | -    |
| V-6      | 0.032       | A, C                            | 163                                 | -   | -    | -   | -    |
| V-7      | 0.033       | B, C                            | 163                                 | -   | -    | -   | -    |
| V-9      | 0.031       | B, C                            | 163                                 | -   | -    | -   | -    |
| VI-1     | 0.91        | A, B                            | 500                                 | -   | -    | -   | -    |
| VI-2     | 0.34        | A, B                            | 350                                 | -   | -    | -   | -    |
| VI-11    | 0.20        | -                               | 275                                 | -   | -    | -   | -    |

#### IV. ANALYSIS

During a burst, temperature data were obtained from 10 to 13 particles and recorded on cards for computer analysis. Bare particle response was used to determine pulse shape. By comparison of the calculated response of the pyrocarbon coated particle and observed response for various assumed values of thermal conductivity, the thermal conductivity which gave the best fit was selected.

##### Mathematical Basis

The energy balance given by Eq. (1) was used for analysis. It was assumed that each coated particle was spherically symmetric and that the thermal energy flowed only in a radial direction. The boundary conditions between the contiguous regions as given by Eqs. (4) and (5) were used.

Convection heat transfer, as defined by Eq. (6), was chosen as the boundary condition of the outer surface. Radiation heat transfer from the surface is insignificant at the experiment temperatures (20 to 300°C).

The energy balance for a spherical particle with an energy source is<sup>(15)</sup>

$$\rho C_p \frac{\partial T}{\partial t} = k \frac{1}{r^2} \frac{\partial}{\partial r} \left( r^2 \frac{\partial T}{\partial r} \right) + Q(t) \quad (1)$$

subject to the initial condition:

$$t = 0 \quad T = T_0 \quad \text{all } r \quad (2)$$

and boundary conditions:

I. At the particle center:

$$T \equiv \text{finite} \quad (3)$$

II. At the boundary common to two contiguous regions:

$$A. \quad T_i = T_{i+1} \quad (4)$$

$$B. \quad k_i \frac{\partial T_i}{\partial r} = k_{i+1} \frac{\partial T_{i+1}}{\partial r} \quad (5)$$

III. At the outer surface:

$$q = -k \frac{\partial T}{\partial r} = h(T - T_{\text{amb}}) \quad (6)$$

The equations were solved in a Crandall<sup>(17)</sup> finite difference form on the CDC 6600 computer.

##### Pulse Shape

The heat generation pulse,  $Q(t)$ , for each reactor burst was derived from the bare uranium carbide particle temperature response. As

recommended by Morrison and Stillman,<sup>(18)</sup> the burst shape was characterized by the equation

$$\frac{dT}{dt} = \frac{Q}{\rho C_p} \quad (7)$$

To eliminate noise in the bare particle data, the integrated normal or Gaussian distribution was fitted to the experimental time-temperature response. Hence, values of temperatures or temperature derivatives could be determined readily for any time,  $t$ . The S-shaped integrated normal distribution given below closely approximated the experimental points. A least-squares optimization program was used for adjusting the five parameters.<sup>(19)</sup>

$$T(t) = P_5 + \frac{(P_4 - P_5)}{\sqrt{2\pi}} \int_{-\infty}^z e^{-\frac{z^2}{2}} dz, \quad (8)$$

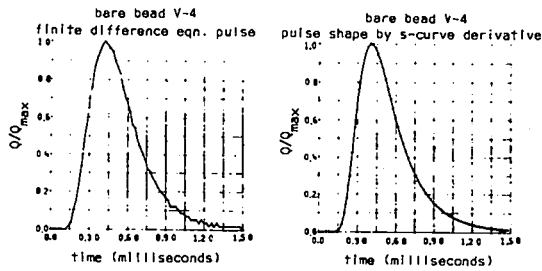
$$\text{where } z = \frac{X - P_1}{\sqrt{P_2 P_3}} \quad (9)$$

The time transformation  $X = \ln(1.25 \ln t + 13.75)$  skewed the curve so that it exhibited a fast rise and a slow tail-off. The derived heat pulse is

$$\frac{Q}{\rho C_p} = \frac{dT}{dt} = \frac{P_4 - P_5}{\sqrt{2\pi}} \frac{1}{(1.25 \ln t + 13.75)} \frac{1.25}{t\sqrt{P_2 P_3}} \text{Exp} \left[ \frac{(X - P_1)^2}{2P_2 P_3} \right] \quad (10)$$

Because the necessary properties were known for the bare  $UC_2$  particles,  $Q(t)$  was calculated directly by an iterative technique using the finite difference equations. Starting at time zero, a value of  $Q$  was assumed and the energy balance was solved for a surface temperature. If the predicted surface temperature did not agree with the temperature obtained from Eq. (8), a new value of  $Q$  was chosen and the procedure repeated until the two temperatures agreed within  $\pm 0.05^\circ\text{C}$ . Normalized pulse shape curves obtained by a rigorous analysis and by a  $dT/dt$  approximation (Fig. 9) were so similar that all pulse shapes used for data reduction were obtained by the faster derivative technique.

Two or three bare particles were monitored during each burst, but a pulse shape derived from only one was used for conductivity calculations. Three criteria were applied consistently in selecting the response curve for the pulse shape (Fig. 10):



1. The fit of the analytical approximation to the response data.
2. The shortest incubation or lag time before a detectable temperature rise.
3. The narrowest pulse.

Small differences in the predicted curves were detectable when the various pulse shapes were used, but those pulses chosen by these criteria produced calculated temperature responses most consistent with experimental data.

Fig. 9. Pulse shape derived by two independent methods.

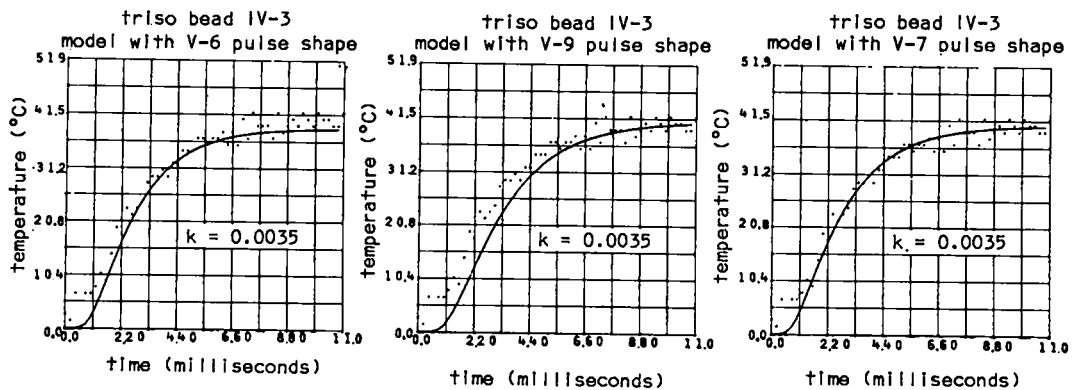
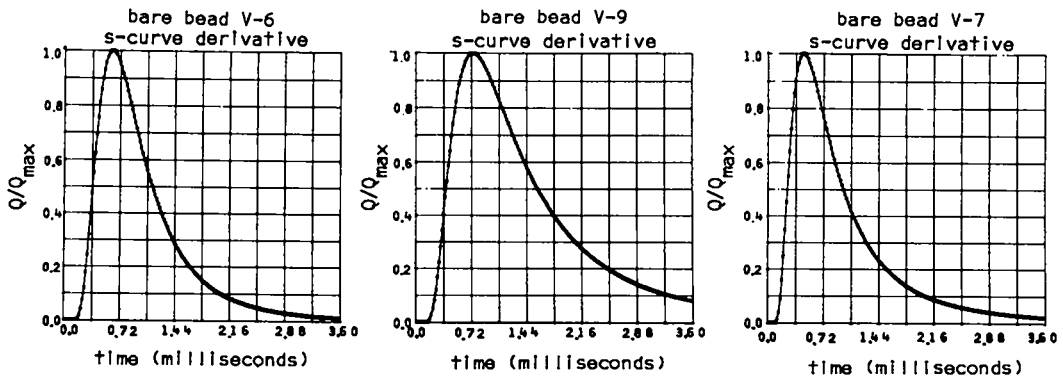
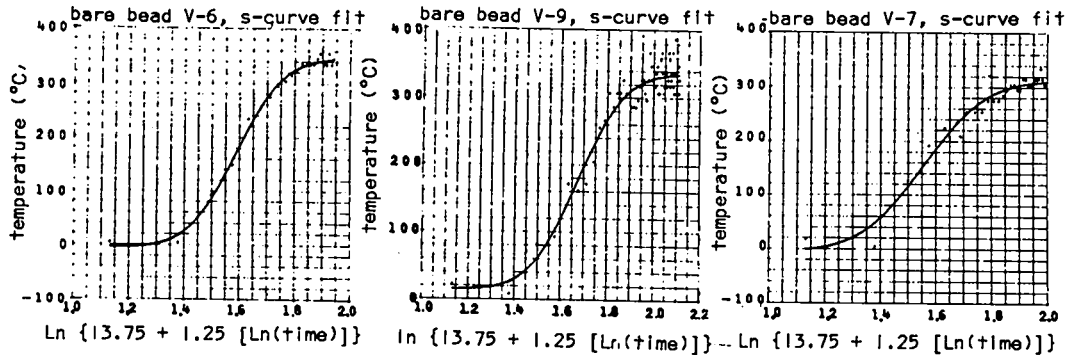


Fig. 10. S-curve fit, pulse shape, and effect on the model of three bare bead responses.

### Surface Heat Transfer Coefficient

The heat transfer coefficient,  $h$ , for a particle was determined from the rate of cooldown observed for the bare uranium carbide particles following a reactor pulse. With the assumption of no heat generation during the cooling period, the coefficient was calculated from the boundary condition Eq. (6), assuming that

$$q = \rho C_p \frac{dT}{dt}$$

for a bare particle. The value of  $h$  was adjusted until the calculation agreed with the observed temperature decline (Fig. 11).

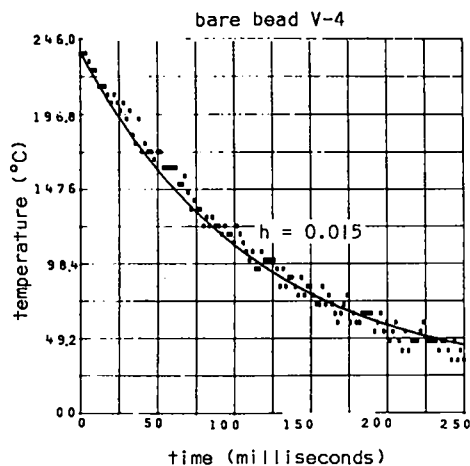


Fig. 11. Cooling curve for heat transfer coefficient calculations.

An effective value for  $h$  of  $0.013 \text{ cal/cm}^2\text{-sec-}^\circ\text{C}$  was determined from bare particle data of 100 and  $200^\circ\text{C}$  bursts. For larger particles,  $h$  was extrapolated by assuming a constant Nusselt number.

### Thermal Conductivity

With a pulse shape and an effective value of  $h$ , pyrocarbon thermal conductivities were determined. In the analysis of Type I, Type II, and Type III particles, two regions, the  $\text{UC}_2$  kernel and the pyrocarbon layer were modeled; the tungsten layer was neglected because of the thin (1 to 3 micron) cross section and because of the high tungsten thermal conductivity ( $0.41 \text{ cal/cm-sec-}^\circ\text{C}$ ). Temperatures at the outside surface of the tungsten were virtually the same as at the pyrocarbon junction. Further, it was desirable to minimize the number of

boundaries since finite difference approximations introduce relatively large errors at these points.<sup>(17)</sup> Four regions were included in the TRISO particle model: the  $\text{UC}_2$  kernel, the buffer layer, the SiC layer, and the isotropic layer.

A small variation of  $k$  caused large changes in the calculated response curve of buffer particles (Fig. 12). The value of  $k$  was varied until a good fit, as determined by observation, was obtained. Typical curves are also shown in Figs. 10 and 13.

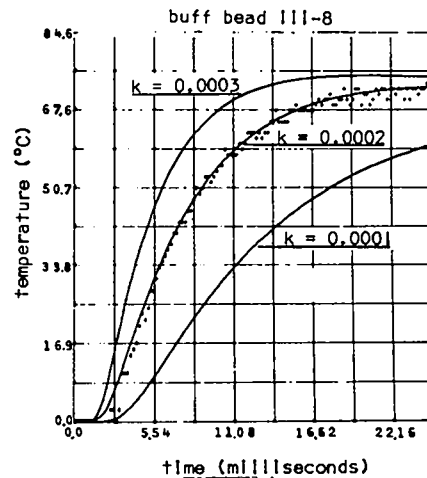


Fig. 12. Effect on the calculated buffer response of varying the thermal conductivity.

A small negative dip occurred in many coated particle response curves before the initial temperature rise. A similar phenomenon had been observed by McEachern. The temperature change of predicted response curves was arbitrarily set equal to the maximum change of the experimental data starting at the minimum temperature of the dip.

### V. RESULTS

Thermal conductivities determined by the fission couple technique were consistent for each particle type. The average thermal conductivity of the isotropic pyrocarbon (Type II) was  $0.009 \pm 0.002 \text{ cal/cm-sec-}^\circ\text{C}$  (Table IV) as compared with GGA's value of  $0.01 \text{ cal/cm-sec-}^\circ\text{C}$  and Wagner's<sup>(6)</sup> value of  $0.020 \text{ cal/cm-sec-}^\circ\text{C}$ . The standard deviation of the isotropic data was  $9.54 \times 10^{-4}$  and no correlation with temperature was observed.

Data from three nonisotropic carbon coated particles (Type I) indicated a conductivity of  $0.002$  to  $0.009 \text{ cal/cm-sec-}^\circ\text{C}$ , compared with Wagner's value of  $0.0038 \text{ cal/cm-sec-}^\circ\text{C}$ .

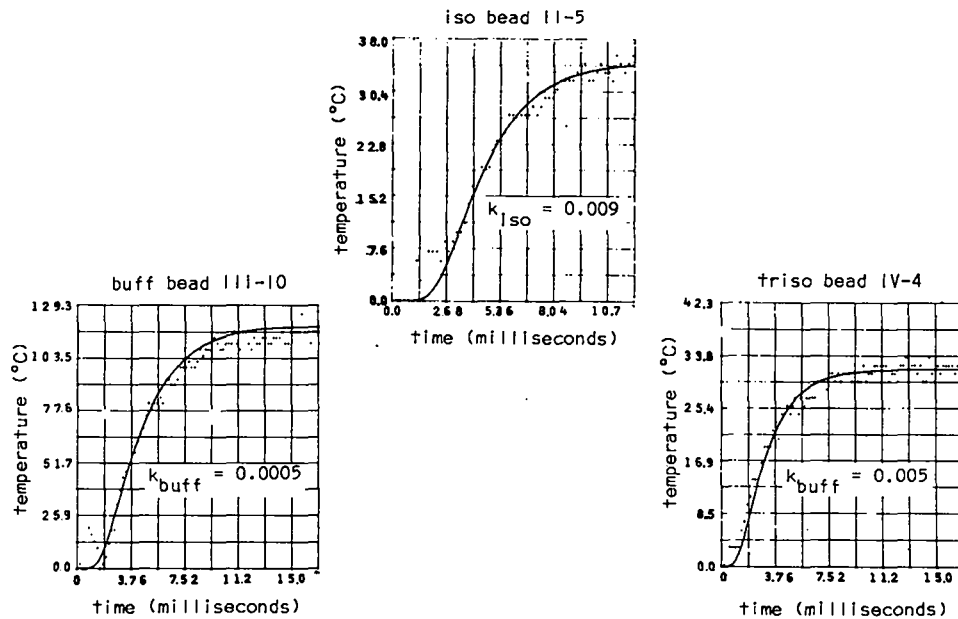


Fig. 13. Examples of the model agreement with experimental data.

The buffer layer conductivity obtained from the Type III particles (Table V) varied with temperature as follows.

$$k_{\text{buff}} = 0.00024 \pm 0.00006 \text{ cal/cm-sec-}^\circ\text{C}$$

for  $50^\circ\text{C} < \Delta T_s < 75^\circ\text{C}$   
and  $\sigma = 0.566 \times 10^{-4}$

$$k_{\text{buff}} = 0.00036 \pm 0.00014 \text{ cal/cm-sec-}^\circ\text{C}$$

for  $75^\circ\text{C} \leq \Delta T_s < 100^\circ\text{C}$   
and  $\sigma = 0.962 \times 10^{-4}$

$$k_{\text{buff}} = 0.00042 \pm 0.00008 \text{ cal/cm-sec-}^\circ\text{C}$$

for  $100^\circ\text{C} \leq \Delta T_s < 200^\circ\text{C}$   
and  $\sigma = 0.753 \times 10^{-4}$

The probability that these thermal conductivity differences were due solely to random variation is between 1.0 and 5.0%.

The experimental responses of the TRISO particles (Type IV) did not agree with the model predictions using conductivity values determined by this method. However, with Wagner's value for isotropic pyrocarbon, the buffer layer conductivity was adjusted until the experimental and predicted curves did agree. The adjusted buffer layer conductivity was  $0.0039 \pm 0.0011 \text{ cal/cm-sec-}^\circ\text{C}$  (Table VI) with a standard deviation of  $6.91 \times 10^{-4}$  and was not effected by temperature. It compares moderately well with GGA's values of 0.0057 and 0.0074 cal/cm-sec- $^\circ\text{C}$ .

## VI. SOURCES OF ERROR

### Code

Precautions were taken to minimize both calculational and experimental errors wherever possible and, where practical, to confirm results by comparison with known values or rough estimates. A calculation confirmed that the surface heat transfer coefficient,  $0.013 \text{ cal/cm}^2\text{-sec-}^\circ\text{C}$ , was a reasonable value for bare particles. Also, a conductivity of  $0.0016 \text{ cal/cm-sec-}^\circ\text{C}$  was obtained for buffer coats from McEachern's data using the computer codes developed for these experiments which incorporated the Crank-Nicholson equations rather than the Crandall equations (Fig. 14). This not only verified McEachern's analysis but ascertained that the code used in this work was free of significant errors.

### Grid

The response of a TRISO bead, which has four coating boundaries, was matched with predicted values from both the Crank-Nicholson and the Crandall equations (Fig. 15); any distinction was undetectable indicating that differences in the discretization errors were unimportant. Results of doubling the number of nodal points from 20 to 40 indicated that errors introduced by the number of lattice lines (30 to 40) in the analysis were small (Fig. 16). If too few nodal points had been used, the large radial increments would cause miscalculations but if too

TABLE IV  
TYPE II PARTICLE THERMAL CONDUCTIVITIES

| Burst | Bead | Reactor Core<br>Temperature<br>Rise $\Delta T_c$<br>(°C) | Particle Surface<br>Temperature Rise,<br>$\Delta T_s$ (°C) | Time<br>Shift<br>(msec) | Calculated Thermal<br>Conductivity, $k_{iso}$<br>(cal/sec-cm-°C) |
|-------|------|--|--|-------------------------|--|
| 755   | II-1 | 149  | 9  | 1                       | 0.01   |
| 756   | II-1 | 149  | 10   | 1                       | 0.01   |
| 757   | II-1 | 205  | 17   | 2                       | 0.007  |
| 757   | II-2 | 205  | 16   | 1                       | 0.008  |
| 758   | II-1 | 294  | 18   | 0.5                     | 0.009  |
| 759   | II-3 | 123  | 18   | 1                       | 0.009  |
| 759   | II-4 | 123  | 17   | 1                       | 0.009  |
| 760   | II-3 | 218  | 34   | 1                       | 0.009  |
| 760   | II-4 | 218  | 33   | 1                       | 0.01   |
| 761   | II-4 | 287  | 40   | 1                       | 0.011  |
| 805   | II-2 | 277  | 37   | 1                       | 0.01   |
| 805   | II-4 | 277  | 39   | 1                       | 0.009  |
| 805   | II-5 | 277  | 31   | 1                       | 0.009  |
| 807   | II-4 | 122  | 15   | 2                       | 0.007  |
| 807   | II-5 | 122  | 12   | 1                       | 0.009  |
| 807   | II-1 | 122  | 12   | 1                       | 0.008  |
| 807   | II-2 | 122  | 15   | 1.5                     | 0.008  |
| 808   | II-2 | 195  | 22   | 1                       | 0.009  |
| 808   | II-5 | 195  | 23   | 1                       | 0.009  |
| 808   | II-4 | 195  | 23   | 1                       | 0.01   |
| 809   | II-2 | 301  | 38   | 0                       | 0.01   |
| 809   | II-5 | 301  | 34   | 1                       | 0.009  |
| 809   | II-1 | 301  | 29   | 1                       | 0.009  |
| 809   | II-4 | 301  | 41   | 1                       | 0.009  |

$k_{iso}(\text{avg.}) = 0.00908$

TABLE V  
TYPE III PARTICLE THERMAL CONDUCTIVITIES

| Burst | Bead   | Reactor Core<br>Temperature<br>Rise $\Delta T_c$<br>(°C) | Particle Surface<br>Temperature Rise,<br>$\Delta T_s$ (°C) | Time<br>Shift<br>(msec) | Calculated Thermal<br>Conductivity, $k_{buff}$<br>(cal/cm-sec-°C) |
|-------|--------|--|--|-------------------------|---|
| 755   | III-7  | 149  | 72   | 2                       | 0.00025   |
| 755   | III-8  | 149  | 57   | 2.5                     | 0.0005  |
| 756   | III-7  | 149  | 72   | 2                       | 0.00025   |
| 756   | III-8  | 149  | 59   | 2                       | 0.00025   |
| 757   | III-7  | 205  | 100  | 1.5                     | 0.00025   |
| 757   | III-8  | 205  | 81   | 2                       | 0.0004  |
| 758   | III-7  | 294  | 158  | 1                       | 0.0004  |
| 758   | III-8  | 294  | 120  | 2                       | 0.0004  |
| 759   | III-11 | 123  | 56   | 0                       | 0.0002  |
| 760   | III-11 | 218  | 99   | 2                       | 0.0005  |
| 761   | III-11 | 287  | 133  | 2                       | 0.0005  |
| 805   | III-8  | 277  | 170  | 2                       | 0.0005  |
| 805   | III-7  | 277  | 170  | 1                       | 0.00035   |
| 805   | III-9  | 277  | 160  | 1                       | 0.0004  |
| 807   | III-8  | 122  | 72   | 2                       | 0.0003  |
| 807   | III-9  | 122  | 68   | 1                       | 0.0002  |
| 807   | III-7  | 122  | 75   | 1                       | 0.0002  |
| 808   | III-8  | 195  | 114  | 1.5                     | 0.00035   |
| 808   | III-9  | 195  | 107  | 1                       | 0.0003  |
| 809   | III-8  | 301  | 185  | 2.7                     | 0.0005  |
| 809   | III-9  | 301  | 170  | 2                       | 0.00035   |
| 809   | III-7  | 301  | 186  | 1                       | 0.00035   |

|                          |            |            |            |
|--------------------------|------------|------------|------------|
|                          | 100° Burst | 200° Burst | 300° Burst |
| $k_{buff}(\text{avg.}):$ | 0.00024    | 0.00036    | 0.00042    |

TABLE VI  
TYPE IV PARTICLE THERMAL CONDUCTIVITIES

| Burst | Bead | Reactor Core Temperature Rise, $\Delta T_c$ ( $^{\circ}\text{C}$ ) | Particle Surface Temperature Rise, $\Delta T_s$ ( $^{\circ}\text{C}$ ) | Calculated Thermal Conductivity, $k_{\text{buff}}$ (cal/cm-sec- $^{\circ}\text{C}$ ) |
|-------|------|--|--|--|
| 755   | IV-1 | 149  | 11.9   | 0.004  |
| 756   | IV-1 | 149  | 13.4   | 0.003  |
| 757   | IV-1 | 205  | 16.3   | 0.004  |
| 758   | IV-3 | 294  | 15.7   | 0.003 (Noisy)  |
| 758   | IV-1 | 294  | 26.5   | 0.003  |
| 759   | IV-5 | 123  | 7.3  | 0.005  |
| 759   | IV-4 | 123  | 10.6   | 0.005  |
| 760   | IV-5 | 218  | 14.9   | 0.003  |
| 760   | IV-4 | 218  | 24.0   | 0.004  |
| 761   | IV-5 | 287  | 22.0   | 0.004  |
| 761   | IV-4 | 287  | 32.0   | 0.0045   |
| 805   | IV-3 | 277  | 36.5   | 0.004  |
| 805   | IV-1 | 277  | 33.7   | 0.005  |
| 807   | IV-1 | 122  | 13.8   | 0.003  |
| 807   | IV-3 | 122  | 14.5   | 0.004  |
| 808   | IV-1 | 195  | 19.4   | 0.004  |
| 809   | IV-1 | 301  | 37.2   | 0.004  |
| 809   | IV-3 | 301  | 40.5   | 0.0035   |

No time shift was required.

$$k_{\text{buff}}(\text{avg.}) = 0.0039$$

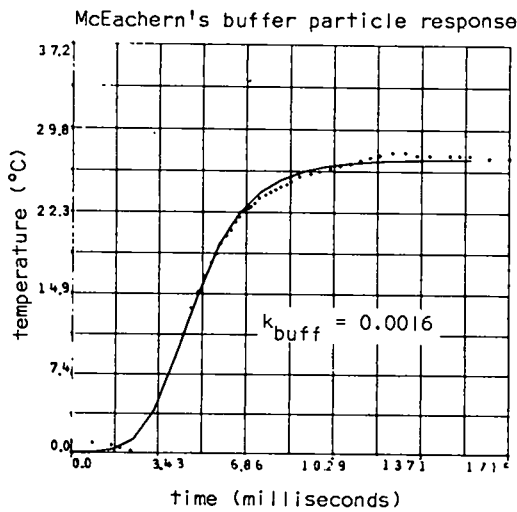


Fig. 14. Model agreement with McEachern's results.

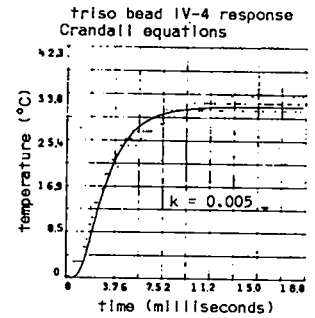
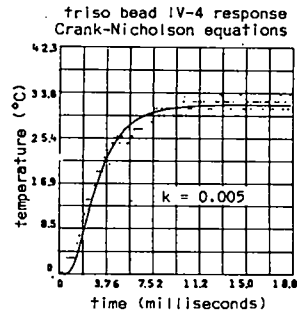


Fig. 15. Model solutions with the Crank-Nicholson equation and with the Crandall equation.

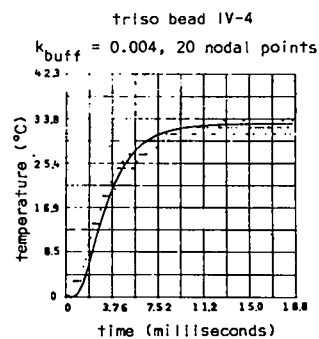
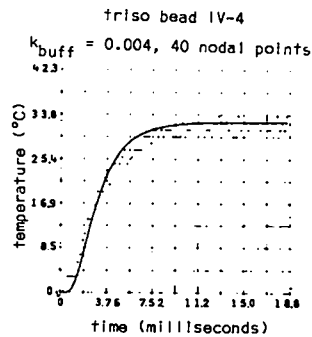


Fig. 16. Effect of doubling the number of nodal points.

many points were used small errors would accumulate. This problem also existed with the time increments. Although the effect of varying the time increment,  $\Delta t$ , was not studied, conductivity differences were not apparent between calculations using 200  $\mu\text{sec}$   $\Delta t$  and those using 1000  $\mu\text{sec}$   $\Delta t$ .

#### Model

The model, a simplification of reality, ignored many phenomena which might have effected the fission couple signal. For example, the response of an intrinsic thermocouple exhibits a measurable lag time. The predicted effective lag time,<sup>(19)</sup> the time to reach 95% of the steady state emf for step forcing, was 20  $\mu\text{sec}$ . Although this was very small when compared with the total response times of 3600.0 to 18000.0  $\mu\text{sec}$ , fission couples were subjected to a pulse rather than a step forcing function and the conductivity measurements depended upon the transient response signal.

#### Deposited Energy

Some gamma-ray energy is deposited in the fuel particle coatings due to pair production, the Compton effect, and the photoelectric effect, but this energy should be less than 1.0% of that deposited in the kernel. Some fission fragments generated near the outer surface of the kernel escape, travel short distances, and deposit their energy in the coating. If a significant amount of heat were generated in the coat, the incubation time would be reduced, but the rate of most of the temperature rise would be unaffected. This is illustrated by a solid line in Fig. 17, which was calculated by assuming uniform heat generation in the buffer layer of a Type III particle equivalent to 3% of the heat generated in the kernel.

#### Electronic Noise

Another source of experimental error is noise introduced by the cables and electronic data recording system. A set of burst experiments was conducted to determine the noise level so that applicable corrections could be made in the response curves. No corrections were necessary. The experiments included two of each of the following thermocouple assemblies, one with a shielded reference junction 10 ft from the reactor and the other with an unshielded reference junction directly above the glory hole as in the fission couple experiments:

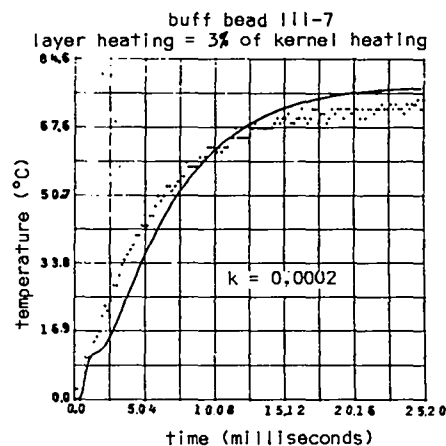


Fig. 17. Effect of heating in the coat.

1. Chromel-constantan thermocouple junction to measure  $\gamma$  heating effects and instrumentation disturbances.
2. Bare copper wire, same purposes as 1.
3. Niobium bead fission couples, same purposes as 1. (Since niobium and tungsten have similar  $\gamma$  cross sections, with appropriate heat capacity corrections, niobium heating may be used as an approximation for tungsten layer heating in the fission couples.)
4. Type III fission couples, control.
5. Type II fission couples, control.
6. Type I fission couples, control.

These assemblies were positioned in the SPR-II core and subjected to neutron bursts as described previously. The surface temperature changes of the control beads were characteristic of similar beads in earlier burst experiments but no noise was detected.

#### Self-Shielding

Self-shielding, in which the neutron flux at the kernel center is reduced by capture near its surface, was considered. A calculation was made to estimate this effect. The heat generation in a buffer particle kernel was confined to an imaginary outer kernel shell with a thickness of one-half the kernel radius. The temperature response was the same as calculated when heat was generated uniformly throughout the kernel.

#### Other Sources

The effect of some other sources of error were studied by McEachern.<sup>(3)</sup> The conductivity measurements were found to be sensitive to errors in the layer thicknesses. Therefore, radial dimensions for the kernel and carbon layers were determined from 100X enlargements of radiographs. The tungsten

layer thickness was measured from a photomicrograph. McEachern also concluded that relatively large errors in the buffer layer heat capacity or in the isotropic pyrocarbon thermal conductivity had little effect on the results. The energy absorbed by these coatings may have affected the maximum surface temperature and the thermal lag time, but they did not change the rate of energy transport. The buffer layer thermal conductivity was much smaller than the isotropic and was the controlling thermal resistance. After the short heat generation period, other particle regions effectively remain in thermal equilibrium.

#### VII. DISCUSSION

The fission couple technique for measuring thermal conductivity of the low-density pyrocarbon buffer coating of a coated fuel particle has been demonstrated. Comparison with independent measurements on two samples of dense pyrocarbon are reasonable and show the validity of the technique. A significant advantage of the fission couple technique is that the measurements are conducted on actual particles rather than on specially prepared material.

The response of a given particle type was found to be consistent. The thermal conductivity measurements made from several different pulses and different particles were reproducible. The following results were obtained.

1. The thermal conductivity of the isotropic pyrocarbon is  $0.009 \pm 0.002$  cal/cm-sec-°C at low temperatures.
2. The thermal conductivity of the buffer material on the TRISO particles is  $0.0039 \pm 0.0011$  cal/cm-sec-°C at low temperatures.
3. The buffer material of the Type III particles may not be the same as that of the TRISO particles. The thermal conductivity of the Type III buffer pyrocarbon is

| Thermal Conductivity<br>cal/cm-sec-°C | Temperature<br>Range, °C |
|---------------------------------------|--------------------------|
| $0.00024 \pm 0.00006$                 | 50 - 75                  |
| $0.00036 \pm 0.00014$                 | 75 - 100                 |
| $0.00042 \pm 0.00008$                 | 100 - 200                |

Two unexplained observations made during the experiments deserve further investigation. The cause of the negative temperature dip has not been identified. The time shift that was used to fit the data has not been justified. The validity of this fitting technique needs further verification.

Dependence of the technique on coating layer thicknesses should be determined. The heat transfer coefficient and dimensional uncertainties become

much more important for small particle size and coating thickness. Heat generation in the coat or other neglected phenomena may also change in significance with layer thickness. The data imply such a relation. Buffer particles analyzed by McEachern had coats 150% thicker than the similar Type III particles and yielded conductivities 375% greater. The TRISO particles with coats 250% thicker yielded conductivities 1000% larger. Conductivity measurements of several particles coated with different thicknesses of the same material should establish this relation.

It is proposed that a set of experiments be made on two different reactor systems. Pulse widths and energy spectrums vary from reactor to reactor and may affect the results. The SPR-II reactor has a 32- $\mu$ sec half-maximum burst pulse width compared with 600  $\mu$ sec for the Super Kukla reactor. It would be desirable to use the same instrumentation for such experiments. If two different instrumentation systems are available, it would be desirable to record a set of experiments with the two systems to investigate instrumentation error.

The temperature dependence of pyrocarbon conductivity should be obtainable. It is suggested that fission couples be heated then be subjected to a low energy pulse. If the procedure is repeated for a series of increasing base temperatures,  $k$  could be correlated with temperature.

#### VIII. ACKNOWLEDGMENTS

The authors acknowledge the contributions of LASL employees R. J. Bard and other members of Group CMB-8 for preparation of particles, C. Fairchild for tungsten coating, D. B. Stillman for his assistance with physics and experimental setup, L. Weintraub for instrumentation and conduct of experiments, and J. R. Payne for fabrication of fission couples. The authors express special thanks to the Sandia Corporation and the SPR-II personnel for their assistance, and for the use of the SPR-II reactor facility. We also thank R. G. Morrison, Phillips Petroleum Company, for assistance in preparation of some fission couples, and Dr. K. L. Holman, New Mexico State University, who, as graduate advisor for G. T. Brock, gave valuable guidance and advice.

IX. REFERENCES

1. W. V. Goeddel, "Coated-Particle Fuels in High-Temperature Reactors: A Summary of Current Applications," Gulf General Atomic, San Diego, California, Nucl. Appl., 3 (October 1967), 599-614.
2. "Summary Report on the Use of TRISO-Coated Particles in the PSC Reactor Plant," Gulf General Atomic, GA-8467 (January 1968).
3. D. W. McEachern, Group K-4, Los Alamos Scientific Laboratory, Los Alamos, New Mexico, internal LASL memorandum (April 14, 1967).
4. K. B. Larson and K. Koyama, "Measurement by the Flash Method of Thermal Diffusivity, Heat Capacity, and Thermal Conductivity in Two-Layer Composite Samples," Gulf General Atomic, GA-6856 (December 29, 1965).
5. W. V. Goeddel and R. G. Mills, Gulf General Atomic, Private Communication (January 11, 1968).
6. P. Wagner, Group CMF-13, Los Alamos Scientific Laboratory, Private Communication (September 9, 1968).
7. W. J. Parker, R. J. Jenkins, C. P. Butler, and G. L. Abbott, "Flash Method of Determining Thermal Diffusivity, Heat Capacity, and Thermal Conductivity," J. Appl. Phys., 32, 9. (September 1961), 1679-1684.
8. R. D. Cowan, Private Communication (August 22, 1968).
9. P. Wagner, Group CMF-13, Los Alamos Scientific Laboratory, Private Communication (March 7, 1968).
10. R. J. Bard, Group CMB-8, Los Alamos Scientific Laboratory, Private Communication (June 21, 1968).
11. R. J. Bard, Group CMB-8, Los Alamos Scientific Laboratory, Private Communication (January 17, 1969).
12. R. J. Bard, Group CMB-8, Los Alamos Scientific Laboratory, Private Communication (January 31, 1967).
13. C. I. Fairchild, J. P. Bertino, W. J. McCreary, and P. G. Salgado, Los Alamos Scientific Laboratory, Private Communication (February 1968).
14. R. L. Coats and P. D. O'Brien, Sandia Laboratory, Albuquerque, New Mexico, "SPR II Safety Analysis Report," SC-44-66-2706 (January 1967).
15. R. L. Long, "Reactivity Contributions in the Glory Hole of the Sandia Pulsed Reactor II," Sandia Laboratory, SC-CR-58-3571 (May 1968).
16. R. B. Bird, W. E. Stewart, and E. N. Lightfoot, Transport Phenomena, (John Wiley and Sons, New York, 1960).
17. R. C. Campbell, B. Kaplan, and A. H. Moore, "A Numerical Comparison of the Crandall and the Crank-Nicholson Implicit Methods for Solving A Diffusion Equation," Trans ASME, Series C, J. Heat Transfer, 88, (August 1966) 324-326.
18. R. G. Morrison and D. B. Stillman, "Fission Couples Applied Toward Reactor Diagnostics and Safety," Los Alamos Scientific Laboratory, LA-3470-MS (January 15, 1966).
19. R. H. Moore and R. K. Zeigler, "The Solution of the General Least Squares Problem with Special Reference to High-Speed Computers," Los Alamos Scientific Laboratory, LA-2367 (October 15, 1959).